Electrocoagulation in Wastewater from Spent-Batteries Recycling

Fika Rofiek Mufakhir[1,2*], Chusnul Khotimah[3], Soesaptri Oediyani[3], Widi Astuti[1], Slamet Sumardi[1], Hendra Prasetia[1], La Ode Arham[2], Hafid Zul Hakim[2], Himawan Tri Bayu Murti Petrus[4], and Venny Poernomo[5]

[1]*Research Center for Mining Technology, National Research and Innovation Agency (BRIN), Jl. Ir. Sutami Km. 15 Tanjung Bintang, Lampung Selatan 35361, Indonesia*

[2]*Department Mining Engineering, Institut Teknologi Sumatera, Jl. Terusan Ryacudu, Way Huwi, Jati Agung, Lampung Selatan 35365, Indonesia*

[3]*Department Metallurgy Engineering, Universitas Sultan Ageng Tirtayasa, Jl. Jenderal Sudirman Km. 3, Kotabumi, Purwakarta, Kota Cilegon, Banten 42435, Indonesia*

[4]*Sustainable Mineral Processing Research Group, Department of Chemical Engineering, Faculty of Engineering, Universitas Gadjah Mada, Jl. Grafika No. 2, Yogyakarta 55281, Indonesia*

[5]*PT. Limas Primenergi Lestari, Raya Bangsalsari, Trisnogambar, Jember 68154, Indonesia*

Abstract: *This study uses electrocoagulation to investigate reducing heavy metal content in wastewater from discharging spent batteries. ICP-OES analysis shows that heavy metals exceed the environmental water standard. The electrocoagulation procedure was conducted within a reactor with a 500 mL volume and a rectifier with a 5 A current capacity. Three types of electrode material combinations were used: iron (Fe) and aluminium (Al) as well as Fe-Fe, Al-Al, and Fe-Al pairs with 1 cm in the distance by parallel monopolar cells. Alternating current was used with 30, 40, and 50 A/m² current density. The best result shown in the Fe-Al electrode pair combination system at 40 A/m² for 30 min contact time and removal efficiencies for Co, Cd, Ni, Zn, and As is 98.76, 90.73, 99.32, 97.93, and 97.78%, respectively, while for Hg it is 31.84%, even though only Cd is above the standard limit. The heavy metal bearing was confirmed using SEM-EDS in the floc and the precipitate residue. The dissolved electrode materials and electrical energy consumed are 0.32 g and 0.109 kWh/m³, respectively. This method can be a good alternative for treating wastewater compared to direct current electrocoagulation, where the electrode and energy will be less consumed.*

Keywords: *alternating current; electrocoagulation; heavy metal; spent-batteries recycling; wastewater*

■ INTRODUCTION

The market for batteries on a global scale is experiencing growth, primarily due to the urgent need to mitigate climate change by transitioning towards battery-powered automobiles and adopting renewable energy sources. The level of lithium-ion (Li-ion) battery consumption in the automotive industry witnessed a significant surge in 2022, experiencing a growth rate of almost 65% to reach a total of 550 gigawatt hours (GWh).

This notable increase can be mainly attributed in response to the increasing sales of electric passenger automobiles, which had a substantial spike of 55% in new registrations during the same period compared to the previous year, 2021 [1]. In Indonesia, the Indonesia Battery Corporation (IBC) is targeting battery production capacity to reach 140 GWh by 2030 [2]. Lithium batteries come in several various types, such as lithium manganese oxide ($LiMn_2O_4$, LMO/spinel),

lithium iron phosphate (LiFePO$_4$, LFP), lithium cobalt oxide (LiCoO$_2$, LCO), and lithium mixed nickel-manganese-cobalt oxide (LiNi$_{1-y-z}$Mn$_y$CO$_z$O$_2$, NMC) [3-5]. Other types of batteries are often found, such as the nickel type: metal hydride, iron, zinc, hydrogen, cadmium (Ni-MH, Fe, Zn, H, Cd), lead acid (Pb), zinc chloride (Zn-Cl), mercury-zinc (Hg-Zn), and alkaline (Zn, MnO$_2$) [6]. In general, the structure of a battery comprises multiple components, including the anode, cathode, separator, insulating ring, cover, casing, and other relevant elements [6], which consist of not only valuable material but also hazardous content. The next challenge, with the large number and very diverse types of batteries, is how to use the technology to recycle used battery waste using effective, efficient, and environmentally friendly technology.

Many researchers have looked into how to recycle used battery waste using hydrometallurgical and pyrometallurgical methods. However, these two techniques still produce waste in gases, liquids, and solids containing heavy metals and hazardous compounds. Various techniques have been utilized to eliminate heavy metals from liquid waste, including combination of oxidation-precipitation-filtration, bioremediation, supercritical fluid extraction, lime softening, ion-exchange, adsorption, activated carbon, the use of aerated granular filters and other filtration materials [7], membrane processes [8], flotation [9], coagulation [10], flocculation [11], and electrocoagulation-chelation [12].

The electrocoagulation method is a promising alternative for treating liquid waste generated while processing spent batteries. This approach possesses numerous benefits. The treatment process has a moderate operation rate, which lets large volumes and higher organic loads be treated. The electroflotation of particles using H$_2$ bubbles allows for this. The process has high efficiency in removing both ionic and colloidal matters. Additionally, the cost of electrodes is relatively low, making it an economically viable option. Furthermore, the process has the potential to operate continuously [13].

Several studies of the process of treating liquid waste originating from battery manufacturing using electrocoagulation reported by Mansoorian et al. [14]

remove the efficiency of lead (Pb) and zinc (Zn) at 96.7 and 95.2%, respectively, at iron electrodes and a current density of 6 mA/cm^2 with an alternating current system. Bhagawan et al. [15] reported that electrocoagulation is a highly effective way to lower heavy metal concentrations in electroplating waste with significant removal rates, with reductions of 96.2% for chromium (Cr), 96.4% for nickel (Ni), 99.9% for zinc (Zn), 98% for copper (Cu), and 99.5% for lead (Pb). In a recent study conducted by Mufakhir et al. [12], it was observed that the implementation of the electrocoagulation process utilizing direct current (DC) exhibited, combined with chelating agents (chitosan and citric acid), a significant reduction of heavy metal (Co, Cd, Ni, Mn, Hg, and As) concentrations in liquid waste battery, surpassing 98%. The utilization of AC in this study was motivated by previous research conducted with DC, which demonstrated that the application of DC can form an oxide layer on the cathode and subsequent anode damage due to oxidation [16]. This phenomenon leads to a reduction in the efficiency of the electrocoagulation process. Consequently, an investigation was conducted utilizing alternating current (AC).

The primary aim of this study was to reduce the levels of heavy metal concentrations, specifically Co, Ni, As, Zn, Cd, and Hg, present in the wastewater generated during the processing of battery recycling. The aim was to ensure the resulting waste met the established environmental water quality standards. By using AC, the study looked at changes in electrocoagulation involves adjusting the amount of current density, electrode material, and contact time. Reduction of the levels of heavy metals, the efficiency of removal, residue analysis, and energy consumption were investigated to ascertain the highly efficient and cost-effective processes.

■ EXPERIMENTAL SECTION

Materials

The materials used in this study included wastewater from the discharge process spent-batteries recycling, aluminum electrode 6061 series, mild steel electrode SS400 series, sandpaper with a coat of 1000 grit, and filter paper (Whatman 42, Assless, Cytiva). The

chemicals used in analytical grade included hydrochloride acid (HCl, 37%, SMART LAB), nitric acid (HNO₃, 65%, Sigma Aldrich), ethanol absolute (C₂H₅OH, ≥ 99.8%, Supelco), and deionized water.

Instrumentation

The experimental equipment in this study included a constance oven, cutting grinder, RP 525 PPS3U AC power supply, and electrocoagulation cell. The analytical instruments used Oakton® pH 450 Waterproof Portable pH meter, Sartorius analytical balance, Deli DL8490 multimeter, Analytical Jena Plasma Quant PQ 9100 Elite inductively coupled plasma-optical emission spectrometry (ICP-OES), Thermo Scientific Quattro S field emission scanning electron microscopy (FESEM) and completed with energy dispersive X-ray spectroscopy (EDS) detector.

Procedure

Experimental setup

The clear, 0.5-mm acrylic used to build the electrocoagulation cell reactor had a 500 mL capacity. The 10 cm × 10 cm × 0.5 cm rectangular shapes were cut using a cutting grinder for the aluminum series 6061 (Al) and the mild steel SS400 Series (Fe). The electrodes were polished with sandpaper, cleaned with 2% ethanol, submerged for 24 h, rinsed with deionized water, and dried at 110 ± 2 °C inside the oven for 2 h. The four electrodes were placed one centimeter apart in a vertical orientation. In a monopolar parallel arrangement, two plates served as cathodes and the other as anodes. The electrodes that provided voltage in the 0–25 V range and electrical current in the 0–5 A field were linked to the AC RP 525 PPS3U power supply. During the electrocoagulation procedure, a constant current was applied without any agitation. The electrode's surface area submerged in the wastewater measured roughly 392 cm.

Experimental procedure

Wastewater (500 mL) from recycled spent batteries was placed into the cell reactor (Fig. 1(a)). The electrodes are installed using three variations: Fe-Fe, Al-Al, and Al-Fe pairs. The current density of 30, 40, and 50 A/m² was achieved by adjusting the AC power supply. Samples of
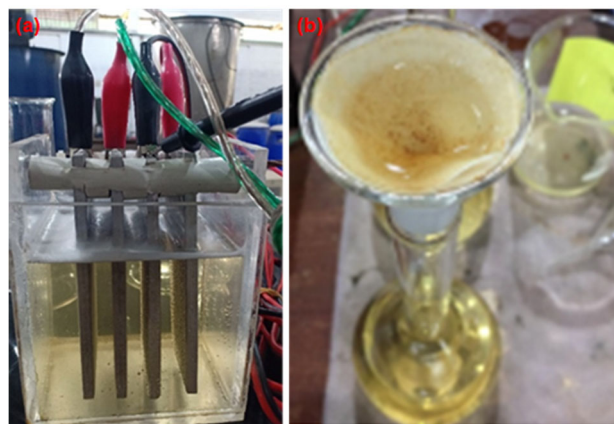

Fig 1. (a) Cell electrocoagulation and (b) filtration

liquid were collected after 10, 20, 30, 40, and 50 min and measured for pH. Filter paper (2.5 µm, Whatman Grade 42) was used to filter the original feed and treated liquid waste samples (Fig. 1(b)). The ICP-OES was used to quantify the concentrations of metal ions present in the filtrate. After gathering the residue, which consists of the flock and precipitate, it was cleaned till the wash water's pH reached 6–7, dried for 6 h at 100 ± 2 °C, and then examined using an FE-SEM. An average outside temperature of about 27 ± 2 °C was used for all test runs. To prevent measurement uncertainty, the experiment was conducted in duplicate.

Calculation

The efficiency of removal (R) was computed by employing the subsequent Eq. (1);

$$R\ (\%) = \frac{CM_0 - CM_t}{CM_0} \tag{1}$$

where the concentrations of the metals (Co, Cd, Ni, Mn, Hg, and As) in the original feed wastewater and the treated liquid waste at a particular time (t) were denoted by CM_0 and CM_t, respectively.

The electric energy consumption per wastewater volume was determined by using the following Eq. (2);

$$E = \frac{tIP}{V} \tag{2}$$

where I stood for direct current (A), P for voltage (V), V for wastewater volume (L), t for contact time (s) in the electrocoagulation process, and E for specific energy usage (kWh/m³).

By using Faraday's law, the amount of dissolved

electrodes a calculation was performed per unit volume of liquid effluent theoretically calculated by using Eq. (3);

$$m = \frac{MwtIt}{VzF} \tag{3}$$

where I was the alternating current (A), t was the electrocoagulation contact time (s), V was the wastewater volume (L), z was the element's chemical equivalent, F was the Faraday constant (96,485 Coulomb/mol), and m was the precise number of dissolved electrodes (g/L).

■ RESULTS AND DISCUSSION

Wastewater Characteristics

Table 1 compares the chemical properties of the wastewater from spent battery recycling used in this experiment to the quality standards specified in Indonesian Government Regulation No. 22 of 2021 for class 4 waters [17]. Table 1 shows that the levels of heavy metals like cobalt (Co), cadmium (Cd), nickel (Ni), zinc (Zn), mercury (Hg), and arsenic (As) were much higher than the recommended level. Thus, improper handling and treatment of wastewater will directly damage the environment.

Electrocoagulation Process

Fig. 2(a) shows the condition of the solution, which was bright yellow before the electrocoagulation process took place. The formation of flocs and the subsequent solution's color changes to a cloudy yellow are shown in Fig. 2(b). That can occur due to physical and chemical phenomena in the solution during the process. These phenomena occur when oxidation occurs. As the water molecules are reduced at the negative electrode, hydroxyl ions (OH$^-$) and oxygen and hydrogen gas bubbles are formed. The sacrificial anode acts as a positive ionic coagulant. Subsequently, the ions that have been generated undergo migration towards the electrode with an opposing charge. This migration leads to the instability of the suspension containing pollutants and particulate matter, resulting in the disruption of the emulsion. Adsorption-efficient metal hydroxides are generated through the chemical reaction of positive and hydroxyl ions; these hydroxide molecules aggregate into larger structures that dissolve in solution. Then, pollutants are

absorbed into the hydroxide structure to form larger aggregates, and redox reactions can convert contaminants into less toxic forms. Following this, the aggregate is either floated to the surface by rising oxygen and hydrogen bubbles in the liquid phase or deposited due to its reasonably significant denseness.

The analysis of Fig. 3 reveals that the initial pH was 11.45, but as the electrocoagulation process progressed, the final pH showed a significant decrease, namely 10.34

Table 1. Heavy metal content of wastewater

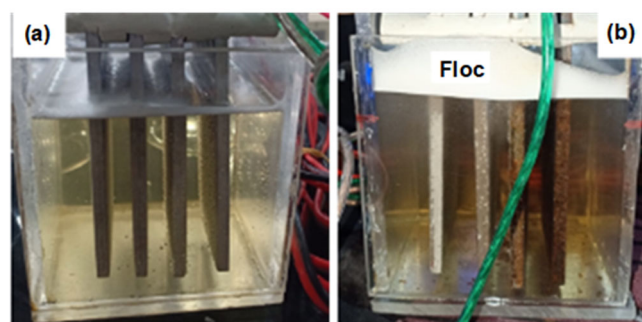| Element (mg/L)	Value (feed sample)	Value (reference)
Co	0.4460	0.200
Cd	0.7800	0.010
Ni	0.7320	0.100
Zn	0.5895	2.000
Hg	0.8803	0.005
As	0.8500	0.100

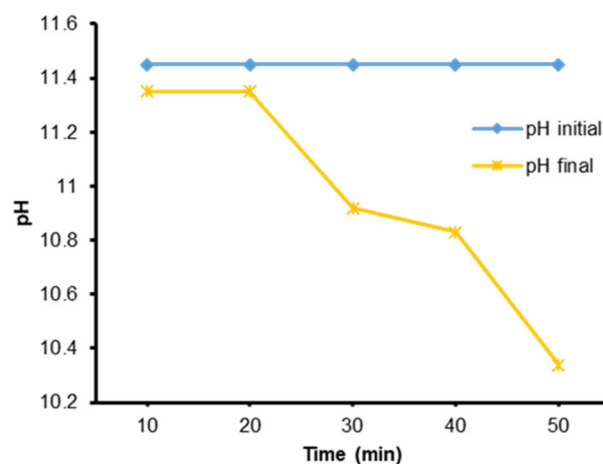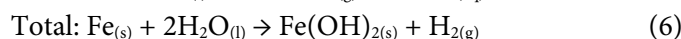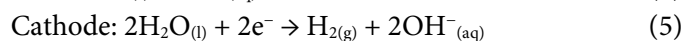**Fig 2.** (a) Before and (b) after electrocoagulation wastewater spent battery recycling

Fig 3. pH characteristic throughout electrocoagulation process

at 50 min. That was caused by H^+ ions increasing while OH^- ions went to bind the floc. Therefore, precipitation also occurs due to charge neutralization and reduced solubility. Due to its AC utilization, the voltage exhibits a fluctuating pattern and is prone to instability. The electrode pair can transition between the anode and cathode poles and vice versa. The following reactions of Eq. (4-6) occur at the Fe electrode.
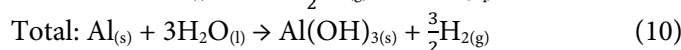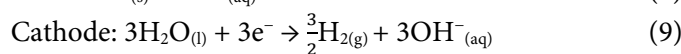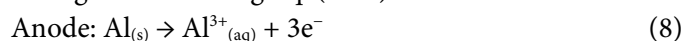
Anode: $Fe_{(s)} \rightarrow Fe^{2+}_{(aq)} + 2e^-$ (4)

Cathode: $2H_2O_{(l)} + 2e^- \rightarrow H_{2(g)} + 2OH^-_{(aq)}$ (5)

Total: $Fe_{(s)} + 2H_2O_{(l)} \rightarrow Fe(OH)_{2(s)} + H_{2(g)}$ (6)

Iron undergoes oxidation in an electrolytic system into Fe^{2+} and Fe^{3+}, resulting in the formation of iron hydroxide. The formation of $Fe(OH)_{n(s)}$ results in the formation of a gelatinous suspension that persists in the aqueous stream. This suspension can remove contaminants from wastewater through coagulation or complexation and electrostatic bond [18]. The pollutant functions as a ligand (L) in the surface complexation phase, chemically binding hydrous iron, showed in Eq. (7).

$L-H_{(aq)} + (OH)OFe_{(s)} \rightarrow L-OFe_{(s)} + H_2O_{(l)}$ (7)

Reactive clusters for water treatment are also formed via the prehydrolysis of Fe^{3+} cations. Fe^{2+} and Fe^{3+} ions are commonly associated with certain ligands (for example, H_2O) and typically exhibit an octahedral form. There are also several identified tetrahedral Fe^{3+} complexes. As a transition metal, Fe^{2+} has an electron configuration of $[Ar]3d^6$, while Fe^{3+} has an electron configuration of $[Ar]3d^5$. Both iron ions possess a minimum of one electron that can be promoted to a higher energy level upon splitting the 3d sub-shell during the interaction and bonding between the core metal ion and ligands. Fig. 4 show the structure model of Fe^{2+} and Fe^{3+} hydroxo complexes, i.e., $Fe(H_2O)_5^{2+}$, $Fe(H_2O)_4(OH)^{2+}$, $Fe(H_2O)_5OH^{2+}$, $Fe(H_2O)_6^{3+}$, $Fe_2(H_2O)_8(OH)_2^{4+}$, and $Fe_2(H_2O)_6(OH)_4^{2+}$.

For the Al electrode, the entailed chemical reactions are arranged as following Eq. (8-10).

Anode: $Al_{(s)} \rightarrow Al^{3+}_{(aq)} + 3e^-$ (8)

Cathode: $3H_2O_{(l)} + 3e^- \rightarrow \frac{3}{2}H_{2(g)} + 3OH^-_{(aq)}$ (9)

Total: $Al_{(s)} + 3H_2O_{(l)} \rightarrow Al(OH)_{3(s)} + \frac{3}{2}H_{2(g)}$ (10)

Analysis of the pE–pH equilibrium diagram demonstrates the presence of different types of charged
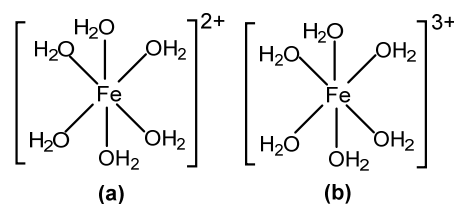
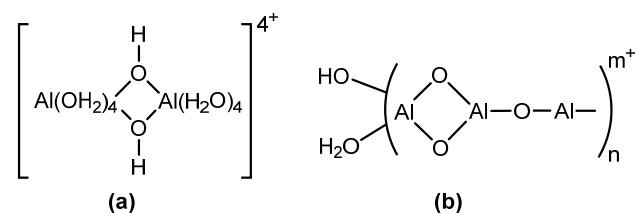**Fig 4.** Structure model of (a) Fe^{2+} and (b) Fe^{3+} hydroxo complexes

Fig 5. Structure model of Al^{3+} (a) dimeric and (b) polymeric

multimeric hydroxyl Al^{3+} species that can be generated under appropriate conditions. The charge neutralization process can be achieved by tangling in a precipitate and adsorbing. However, it is essential to note that the system may also contain additional ionic species, including $Al(OH)^{2+}$, $Al_2(OH)^{5+}$, and $Al(OH)_4^-$, which are influenced based on the pH of the water-based solution. These hydroxo-cationic-charged gelatinous compounds are capable of efficiently eliminating contaminants. The monomeric species classified as cationic (Al^{3+}, $Al(OH)^{2+}$) are generated under low pH conditions. They undergo an initial transformation at the right pH level into $Al(OH)_3$ and subsequently undergo polymerization to become $Al_n(OH)_{3n}$. Fig. 5 shows the configurations of Al^{3+} hydroxo complexes that are dimeric and polymeric.

Effect of Current Density at Variations of Electrode Pairs

Fig. 6-8 show Co, Cd, Ni, Zn, Hg, and As concentration reduction with different current densities at Al-Al, Fe-Fe, and Fe-Al electrode pairs, respectively. Only Co and Hg can be reduced below environmental quality standards at the Al-Al electrode pair. At Fe-Fe, only Cd and Zn cannot be reduced effectively. All heavy metals, except Cd, can be reduced below environmental quality standards in all current density applications at the Fe-Al electrode pair. The 40 and 50 A/m^2 current densities at 30 min give the best results. That leads to the

number of oxidized metal ions increasing at higher currents, which favors a decrease in heavy metal levels by forming more precipitates [19-20]. That can also occur because of the correlation with the contact time, further reducing the heavy metal levels [21]. Nevertheless, this does not significantly affect Cd, based on existing research, it has been shown that the pH of cadmium precipitation typically commences at a value of 8.2 [22]

and the efficacy of this elimination mechanism is particularly pronounced in cases where the pH level is significantly low within an acidic solution [23]. Consequently, higher pH levels result in diminished removal efficacy. Under conditions of low pH, the Cd^{2+} ions were required to engage in competition with H^+ ions in order to occupy adsorption locations on the adsorbent's surface. As the pH level was elevated, the
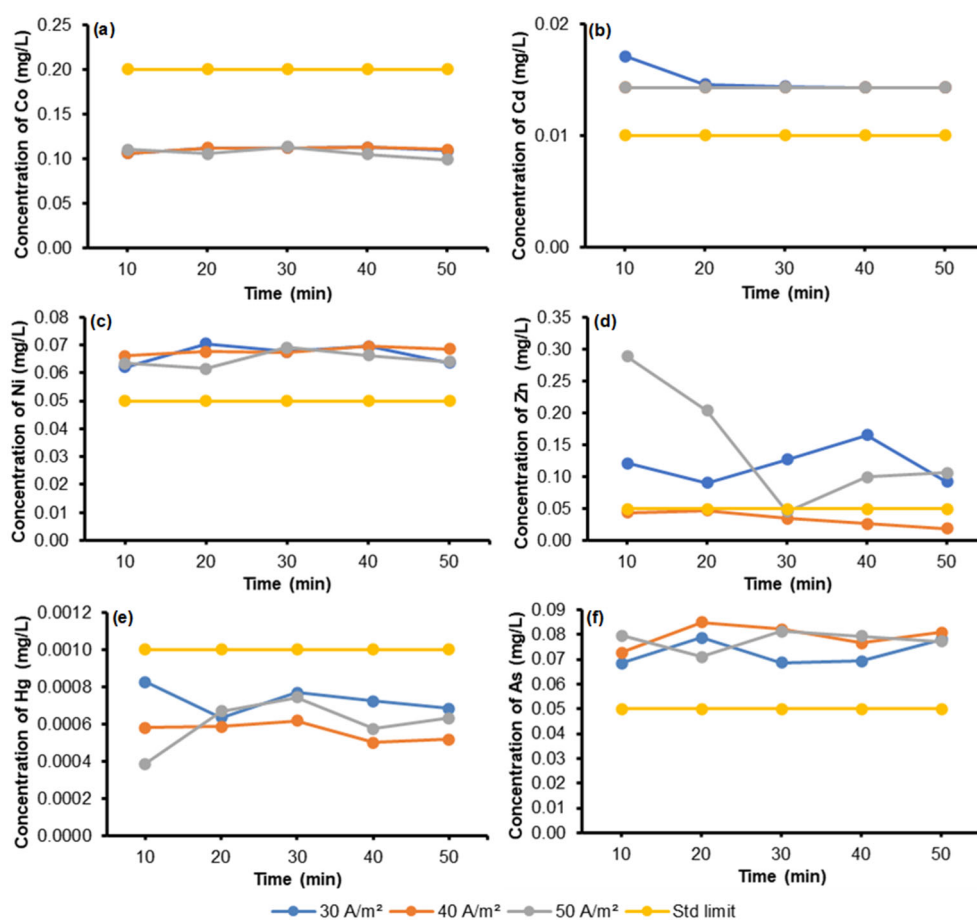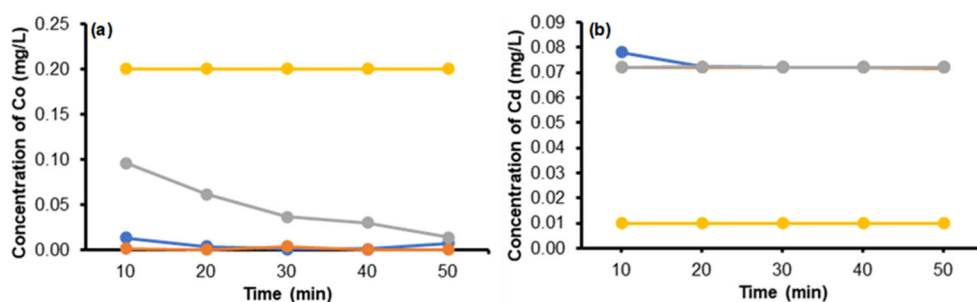

Fig 6. Effect of current density on concentration decrease of (a) Co, (b) Cd, (c) Ni, (d) Zn, (e) Hg, and (f) As as function of time (experimental condition: electrode pair of Al-Al; inter-electrode distance of 1 cm)
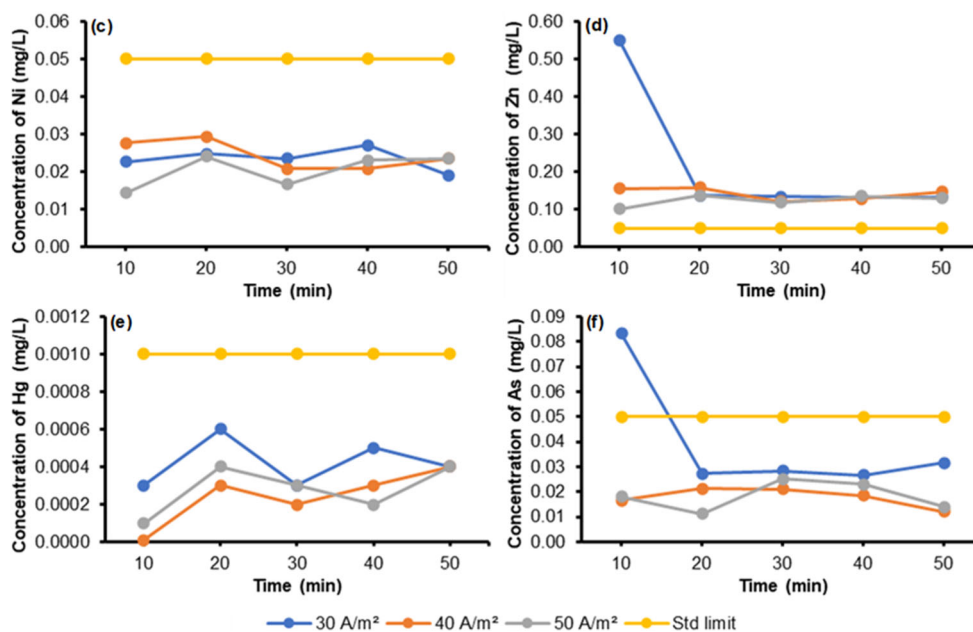
Fig 7. Effect of current density on concentration decrease of (a) Co, (b) Cd, (c) Ni, (d) Zn, (e) Hg, and (f) As as function of time (experimental condition: electrode pair of Fe-Fe; inter-electrode distance of 1 cm)
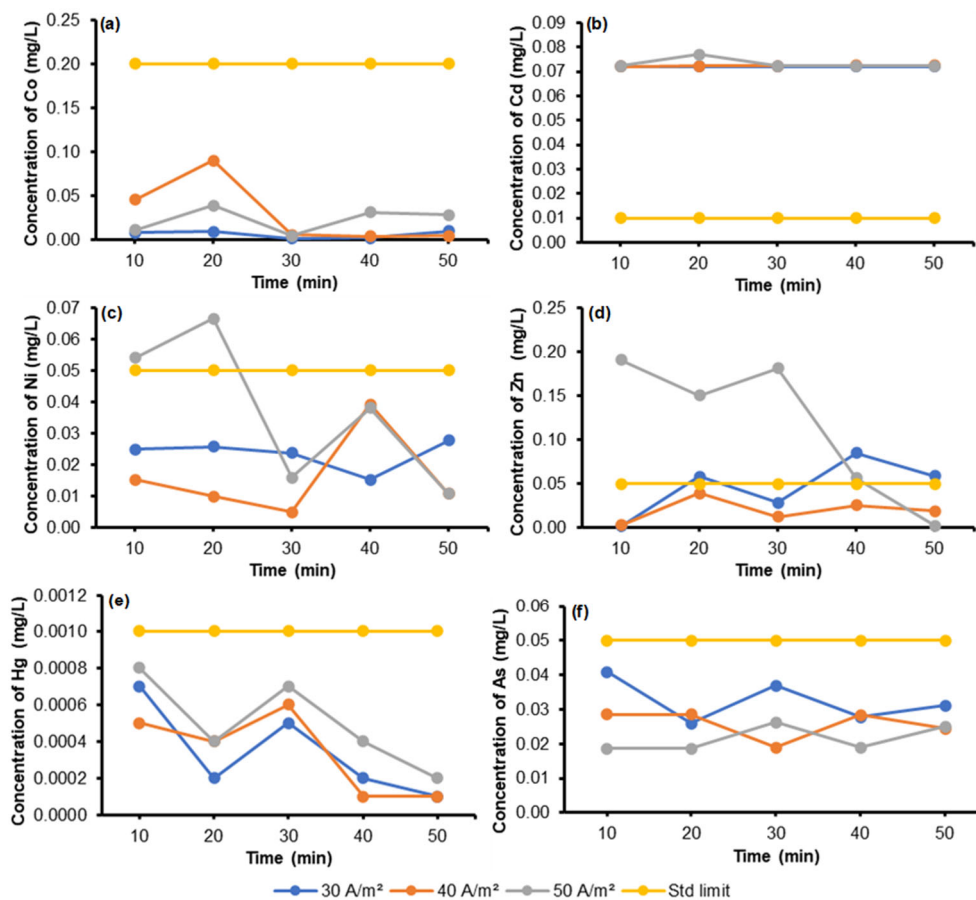

Fig 8. Effect of current density on concentration decrease of (a) Co, (b) Cd, (c) Ni, (d) Zn, (e) Hg, and (f) As as function of time (experimental condition: electrode pair of Fe-Al; inter-electrode distance of 1 cm)

intensity of this competition diminished, resulting in a greater influx of Cd^+ ions replacing H^+ ions that were previously attached to the adsorbent surface.

Fig. 9 shows the solubility of metal (Co, Cd, Ni, Zn, Hg, and As) hydroxides as a function of pH [24-27]. The transformation of a substance from an ionic species to its hydroxide precipitate state is significantly impacted by its concentration in the solution and the pH level. Metal hydroxides exhibit amphotericity, making them more soluble at low and high pH levels. The point of minimal solubility, the optimal pH for precipitation, varies for each metal. The solubility of one metal hydroxide may be low at a specific pH, while the solubility of another metal hydroxide may be comparatively high. Due to their high solubility, metal hydroxides tend to revert into the solution at even minor alterations in pH. There is a particular pH at which the best hydroxide precipitation happens for each dissolved metal. As though for Ni at pH 10.8, for Zn at pH 10.1 [28], for Co at pH 12 [29], for $Hg(OH)^+$ at pH 4.5, for $Hg(OH)_3^-$ at pH 13.2 [30], and As at pH 9.9 [31]. The pH value of this substance is notably similar to the pH level observed in wastewater generated from the recycling of spent batteries. At optimal conditions, the dotted line displays shift in heavy metal concentrations before and after electrocoagulation (Fe-Al pair, 40 A/m^2 and 30 min), along with changes in pH. The solubility line of Fe^{3+} crosses the concentration of heavy metals before the electrocoagulation process. It indicates that the formation of Fe-hydroxy complexes can be enhanced, leading to an accelerated precipitation and floc formation rate. In contrast, the solubility line of Al^{3+} is located further away, indicating whether the Fe electrode is superior to the Al electrode at this condition.

Heavy Metal Removal Efficiency

The removal efficiencies were determined using Eq. (1) of Co, Cd, Ni, Zn, Hg, and As, as shown in Fig. 10. It was found that these removal rates went up when the Fe-Al electrode pair was used in the electrocoagulation process, no matter what current density was used. As time passes, especially around the 30 min mark, the current flow at the electrode increases. That leads to more $Fe(OH)_2$ and $Al(OH)_3$ being made (Eq. (6) and (10)), which acts as a coagulant. This coagulant effectively binds heavy metals. Furthermore, the production of additional H_2 (Eq. (5) and (9)) gas facilitated the buoyancy of the heavy metals, resulting in their separation from the solution. Furthermore, the Fe-Al
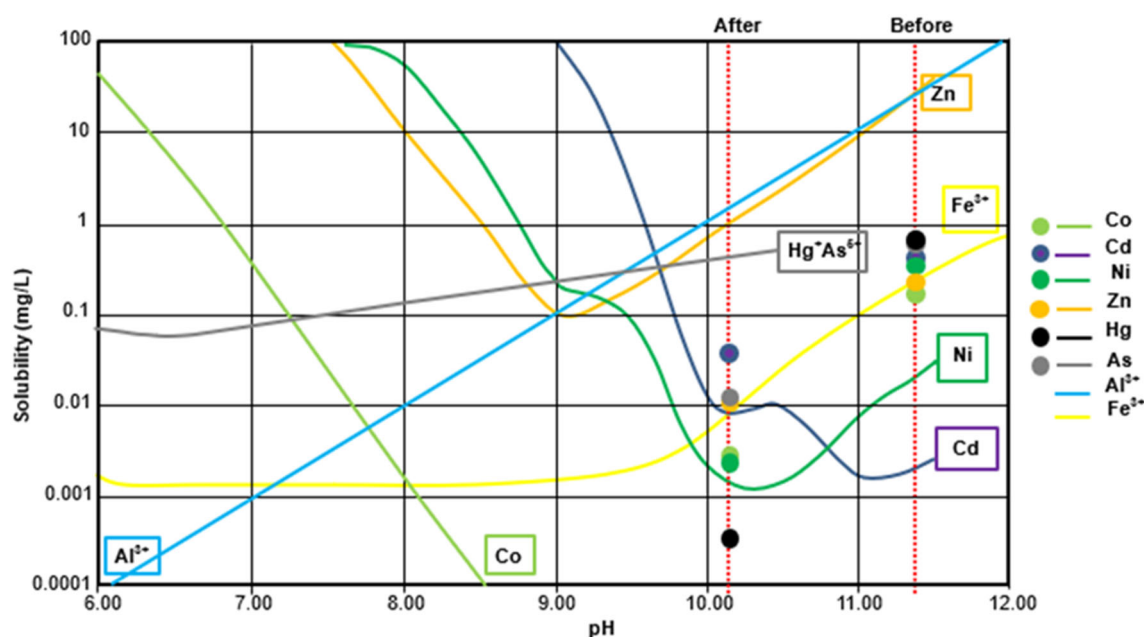

Fig 9. Schematic solubility of metal (Co, Cd, Ni, Zn, Hg, As, Al^{3+}, and Fe^{3+}) hydroxides as a function of pH and the concentration before and after electrocoagulation process
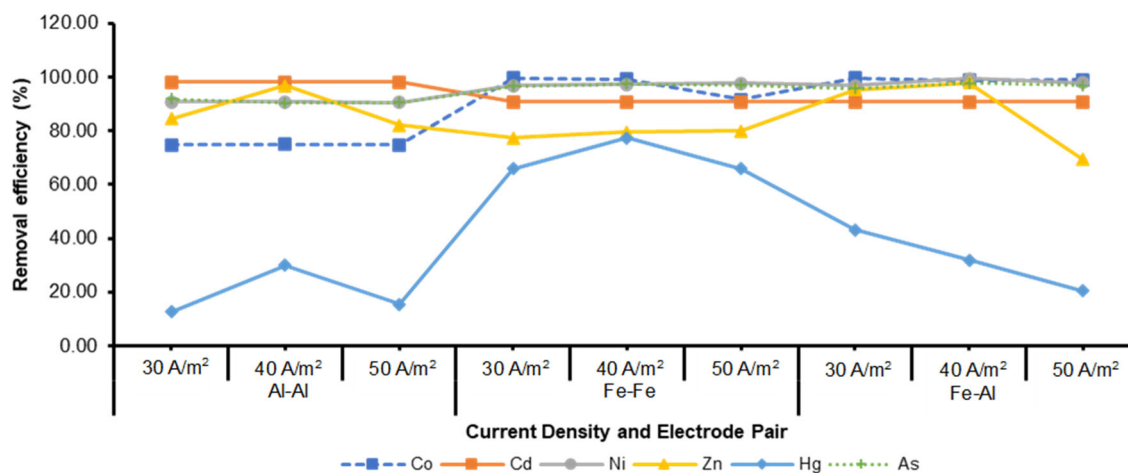
Fig 10. Comparison of the current density and electrode pair on heavy metal removal efficiency (experimental condition: at 30 min)

electrode exhibited a higher efficiency in removing heavy metals than the Fe-Fe and Al-Al electrodes. During electrocoagulation utilizing the aluminium electrode, the anode can release Al^{3+} ions, forming $Al(OH)_3$ flocs. Nevertheless, in the context of employing Fe electrodes, the presence of Fe^{2+} and Fe^{3+} ions can potentially lead to the generation of distinct iron hydroxide species, namely $Fe(OH)_2$ and $Fe(OH)_3$. Consequently, it is necessary to increase the current densities to produce an equivalent quantity of Al^{3+} ions at the aluminium anode, as opposed to the Fe^{2+} and Fe^{3+} ions formed at the iron anode. Iron anodes have a higher ability to produce metal hydroxides with the same current density, leading to improved metal-removal efficiency [32]. This significant effect can be seen in Hg, where the Fe electrode provides a higher removal efficiency than the Al electrode.

Residue Analysis

Residue analysis is employed to identify the constituent materials transported throughout the filtration or flotation procedure using SEM-EDS. The residue comprises a conglomerate of precipitates created due to flocculation, which occurs when a coagulant is introduced during electrocoagulation. Simultaneously, the suspended particulate matter is analyzed to ascertain the existence of heavy metal constituents within it.

Fig. 11 shows the difference in shape and size between precipitates and floc. Precipitates resemble lumps with an irregular shape and are approximately 20 μm in diameter, while flocs are aggregated with elongated-like short rods and under 7 μm in length. This difference can occur due to the precipitation of heavy metals into their larger metal hydroxides. Simultaneously,
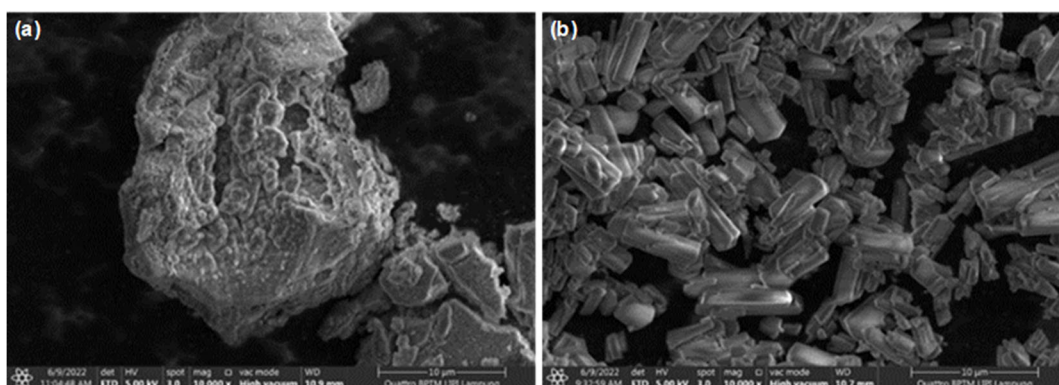

Fig 11. SEM morphological analysis of (a) precipitate and (b) floc at 10,000× magnification
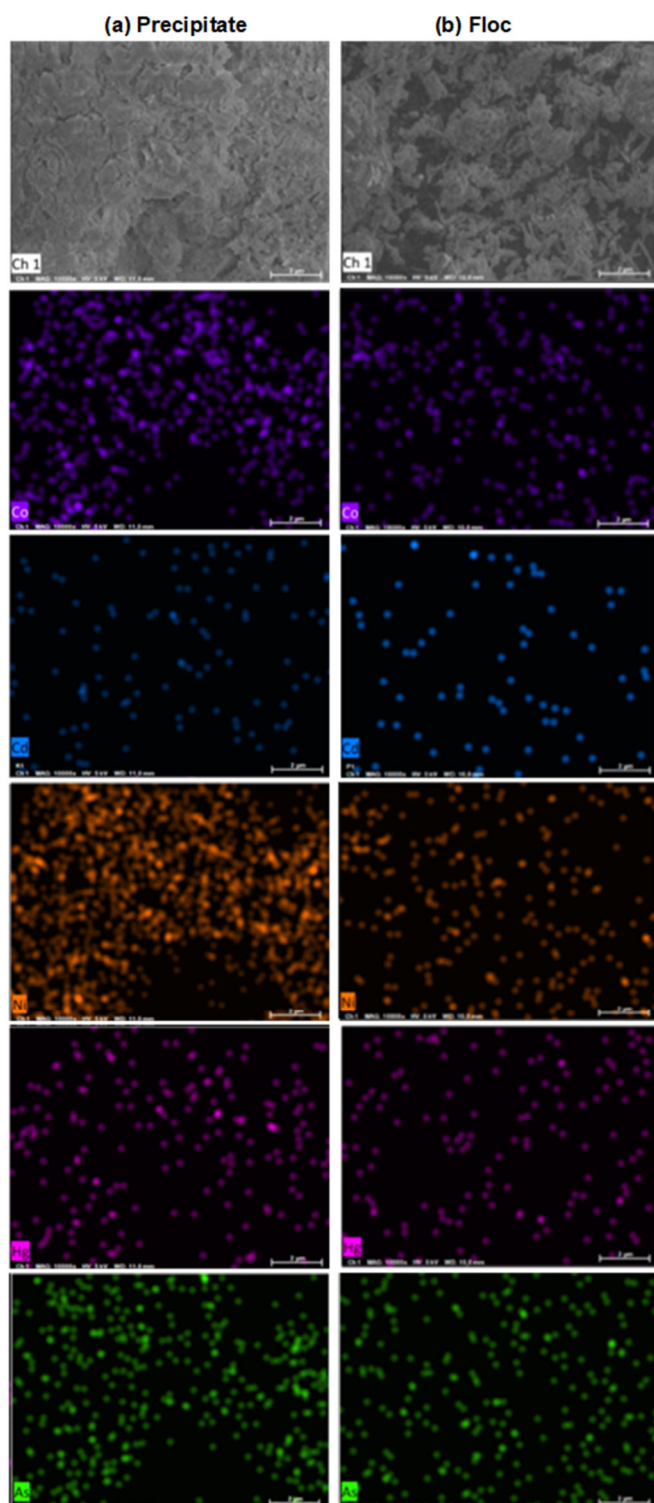
Fig 12. SEM EDS mapping of the (a) precipitate and (b) floc

hydrogen gas is emitted as a result of the water reduction process occurring at the cathode, making it easier for

small particles in the form of floc to move through the flotation process. This morphological shape and size differ from the precipitate and floc produced by general chemical coagulation [33-36] and electrocoagulation methods [37-40]. Due to differences in the growth processes of precipitate and floc through the electrocoagulation process. Parameters that influence such as type of pollutant, species and concentration of heavy metals in solution and process conditions during electrocoagulation. The main factors included electrocoagulation cell design, power supply, electrode/coagulant material, electrode formation, time, pH, current density, temperature, conductivity, mixing pattern [41-42]

Fig. 12 compares the distribution of heavy metals, such as Co, Cd, Ni, Hg, and As, in the precipitates and floc. Both substances consist of heavy metals and exhibit distinct distributions, with flocs being less abundant and more widely spread out than precipitates. At precipitate, As and Ni element distribution looks denser than other heavy metals such as Co, Cd, and Hg. The floc contains heavy metal elements, with their distribution more scattered. That confirms that the levels of the heavy metal elements that will be reduced are more settled into a precipitate than trapped in the gas so that they float and become floc.

Table 2 shows heavy metals' mass and atomic ratio between precipitates and floc. In the precipitates, it was confirmed that the mass of As metal was greater than that of other metals, namely 6.07%. Meanwhile, the mass of heavy metals within the floc is relatively insignificant; the most significant concentration is 0.26% Cd. Only Zn metal was not detected in either residue.

Dissolved Electrodes and Energy Consumption

A certain number of dissolved electrodes and the energy consumption throughout the experiment are depicted in Fig. 13 using Eq. (2) and (3). Heavy metal ion removal's efficacy positively correlates with a specific number of electrodes has been dissolved, resulting in energy consumption in the waste [43]. This correlation is strengthened when the current density and contact time are increased. With 40 A/m² of current density, the
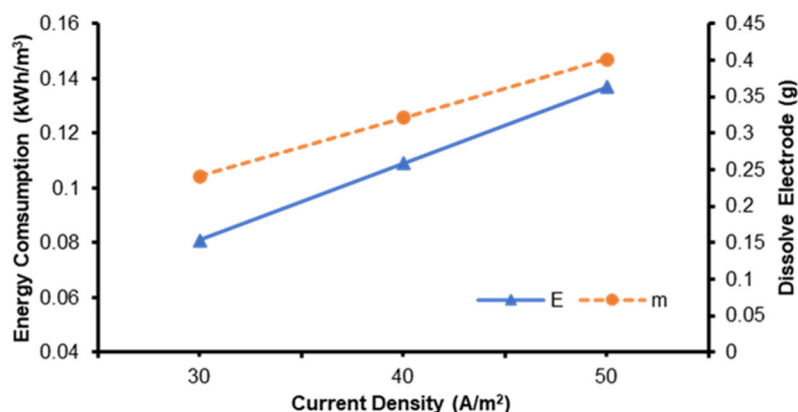
Fig 13. Correlation of dissolved electrodes and energy consumption during the 30 min electrocoagulation process (E = energy consumption, m = dissolved electrode)

Table 2. Comparison of quantification results of SEM-EDS analysis of the precipitates and flocs

Elements	Precipitate		Floc	
	Mass (%)	Atom (%)	Mass (%)	Atom (%)
Cd	1.33	0.23	0.26	0.13
As	6.07	1.60	0.08	0.02
Hg	0.16	0.05	0.06	0.01
Co	0.18	0.02	0.01	0.00
Ni	1.07	0.38	0.00	0.00

best condition for energy consumption is 0.109 kWh/m^3 and 0.32 g of dissolved electrodes for 30 min. Based on previous research conducted by Mufakhir et al. [12], using DC with the addition of chitosan chelating agent consumed 0.1740 kWh/m^3 of energy and dissolved electrodes of 0.4263 g, when compared with data from the electrocoagulation process carried out with AC. The results show that the energy consumption in AC and the number of dissolved electrodes is lower than using DC. This analysis implies that utilizing AC is regarded as more efficient in relation to energy consumption and electrode solubility [44-46].

CONCLUSION

Even though only Cd is above the standard limit, the Fe-Al electrode combination is the optimal choice for removing heavy metal from wastewater from recycled spent batteries with an AC electrocoagulation system. At 40 A/m^2 current density for 30 min contact time, removal efficiencies for Co, Cd, Ni, Zn, and As are 98.76, 90.73, 99.32, 97.93, and 97.78%, respectively, while for Hg is 31.84%. Heavy metal particles removed can be found in the precipitates and the floc. The dissolved electrode materials and electrical energy consumed are 0.32 g and 0.109 kWh/m^3, respectively. The AC electrocoagulation system, one potential solution for the removal of heavy metals from liquid waste, is a viable option for spent battery recycling.

ACKNOWLEDGMENTS

CONFLICT OF INTEREST

The authors do not have a conflict of interest in disclosure. All co-authors have seen and agree with the consent of the manuscript.

AUTHOR CONTRIBUTIONS

Fika Rofiek Mufakhir conceived of the presented idea. Fika Rofiek Mufakhir, and Soesaptri Oediyani developed the theory conception and design of the study. Widi Astuti and Slamet Sumardi performed the analysis. Hendra Prasetia and Himawan Tri Bayu Murti Petrus verified the analytical methods. Chusnul

Khotimah and Slamet Sumardi conducted material preparation and data collection. Venny Poernomo supplied the spent lithium-ion batteries. The results were collectively evaluated and interpreted by Fika Rofiek Mufakhir, Widi Astuti, La Ode Arham, as well as Hafid Zul Hakim. Fika Rofiek Mufakhir, Soesaptri Oediyani, and Chusnul Khotimah drafted the initial version of the paper. Fika Rofiek Mufakhir was responsible for the editing and final manuscript. All authors reviewed the results and approved the final version of the manuscript.

■ REFERENCES

[1] International Energy Agency, 2023, *Global EV Outlook 2023: Catching up with climate ambitions*, OECD Publishing, Paris.

[2] Meilanova, D.R., 2021, *IBC Targetkan Produksi Baterai hingga 140 GWh pada 2030*, https://ekonomi.bisnis.com/read/20210326/44/1373074/ibc-targetkan-produksi-baterai-hingga-140-gwh-pada-2030, accessed on March 13, 2024.

[3] Randau, S., Weber, D.A., Kötz, O., Koerver, R., Braun, P., Weber, A., Ivers-Tiffée, E., Adermann, T., Kulisch, J., Zeier, W.G., Richter, F.H., and Janek, J., 2020, Benchmarking the performance of all-solid-state lithium batteries, *Nat. Energy*, 5 (3), 259–270.

[4] Cheng, X.B., Liu, H., Yuan, H., Peng, H.J., Tang, C., Huang, J.Q., and Zhang, Q., 2021, A perspective on sustainable energy materials for lithium batteries, *SusMat*, 1 (1), 38–50.

[5] Cheng, Z., Liu, T., Zhao, B., Shen, F., Jin, H., and Han, X., 2021, Recent advances in organic-inorganic composite solid electrolytes for all-solid-state lithium batteries, *Energy Storage Mater.*, 34, 388–416.

[6] European Commission, Joint Research Centre, Ciuta, T., Georgitzikis, K., Pennington, D., Mathieux, F., Huisman, J., and Bobba, S., 2020, *RMIS, Raw Materials in the Battery Value Chain – Final Content for the Raw Materials Information System – Strategic Value Chains – Batteries Section*, Publications Office of the European Union, Luxembourg.

[7] Muralikrishna, I.V., and Manickam, V., 2017, "Wastewater Treatment Technologies" in *Environmental Management*, Eds. Muralikrishna, I.V., and Manickam, V., Butterworth-Heinemann, Oxford, UK, 249–293.

[8] Obotey Ezugbe, E., and Rathilal, S., 2020, Membrane technologies in wastewater treatment: A review, *Membranes*, 10 (5), 89.

[9] Peleka, E.N., Gallios, G.P., and Matis, K.A., 2018, A perspective on flotation: A review, *J. Chem. Technol. Biotechnol.*, 93 (3), 615–623.

[10] Cui, H., Huang, X., Yu, Z., Chen, P., and Cao, X., 2020, Application progress of enhanced coagulation in water treatment, *RSC Adv.*, 10 (34), 20231–20244.

[11] Maćczak, P., Kaczmarek, H., and Ziegler-Borowska, M., 2020, Recent achievements in polymer bio-based flocculants for water treatment, *Materials*, 13 (18), 3951.

[12] Mufakhir, F.R., Yuliamsa, I.A., Juniarsih, A., Astuti, W., Sumardi, S., Handoko, A.S., Sudibyo, S., Alam, F.C., Arham, L.O., Poernomo, V., and Petrus, H.T.B.M., 2022, Heavy metals removal in liquid waste from spent-batteries recycling, *IOP Conf. Ser.: Earth Environ. Sci.*, 1017 (1), 012004.

[13] Ebba, M., Asaithambi, P., and Alemayehu, E., 2022, Development of electrocoagulation process for wastewater treatment: Optimization by response surface methodology, *Heliyon*, 8 (5), e09383.

[14] Mansoorian, H.J., Mahvi, A.H., and Jafari, A.J., 2014, Removal of lead and zinc from battery industry wastewater using electrocoagulation process: Influence of direct and alternating current by using iron and stainless steel rod electrodes, *Sep. Purif. Technol.*, 135, 165–175.

[15] Bhagawan, D., Poodari, S., Pothuraju, T., Srinivasulu, D., Shankaraiah, G., Yamuna Rani, M., Himabindu, V., and Vidyavathi, S., 2014, Effect of operational parameters on heavy metal removal by electrocoagulation, *Environ. Sci. Pollut. Res.*, 21 (24), 14166–14173.

[16] Mollah, M.Y.A., Schennach, R., Parga, J.R., and Cocke, D.L., 2001, Electrocoagulation (EC) – Science and applications, *J. Hazard. Mater.*, 84 (1), 29–41.

[17] Ministry of State Secretariat of the Republic of Indonesia, 2021, *Peraturan Pemerintah Republik*

Indonesia, Lampiran VI PP No. 22 Tahun 2021, Ministry of State Secretariat of the Republic of Indonesia, Jakarta, Indonesia.

[18] Tahreen, A., Jami, M.S., and Ali, F., 2020, Role of electrocoagulation in wastewater treatment: A developmental review, *J. Water Process Eng.*, 37, 101440.

[19] Khosa, M.K., Jamal, M.A., Hussain, A., Muneer, M., Zia, K.M., and Hafeez, S., 2013, Efficiency of aluminum and iron electrodes for the removal of heavy metals [(Ni (II), Pb (II), Cd (II)] by electrocoagulation method, *J. Korean Chem. Soc.*, 57 (3), 316–321.

[20] McBeath, S.T., Nouri-Khorasani, A., Mohseni, M., and Wilkinson, D.P., 2020, *In-situ* determination of current density distribution and fluid modeling of an electrocoagulation process and its effects on natural organic matter removal for drinking water treatment, *Water Res.*, 171, 115404.

[21] Vepsäläinen, M., and Sillanpää, M., 2020, "Electrocoagulation in the Treatment of Industrial Waters and Wastewaters" in *Advanced Water Treatment*, Elsevier, Amsterdam, Netherlands, 1–78.

[22] Vasudevan, S., Lakshmi, J., and Sozhan, G., 2011, Effects of alternating and direct current in electrocoagulation process on the removal of cadmium from water, *J. Hazard. Mater.*, 192 (1), 26–34.

[23] Colantonio, N., and Kim, Y., 2016, Cadmium(II) removal mechanisms in microbial electrolysis cells, *J. Hazard. Mater.*, 311, 134–141.

[24] David, M., 2017, *Arsenic Removal from Water*, https://www.911metallurgist.com/arsenic-removal-water/, accessed on March 13, 2024.

[25] Lewis, A.E., 2010, Review of metal sulphide precipitation, *Hydrometallurgy*, 104 (2), 222–234.

[26] de Repentigny, C., Courcelles, B., and Zagury, G.J., 2018, Spent MgO-carbon refractory bricks as a material for permeable reactive barriers to treat a nickel- and cobalt-contaminated groundwater, *Environ. Sci. Pollut. Res.*, 25 (23), 23205–23214.

[27] Digital Analysis Corporation, 2019, *Heavy Metal Removal from Industrial Wastewater*, https://www.phadjustment.com/TArticles/Heavy_Metal_Reduction.html, accessed on March 13, 2024.

[28] Water Specialist, 2024, *Recipitation-by-pH*, https://waterspecialists.biz/info-bulletins/precipitation-by-ph/, accessed on March 13, 2024.

[29] Huang, J.H., Kargl-Simard, C., Oliazadeh, M., and Alfantazi, A.M., 2004, pH-Controlled precipitation of cobalt and molybdenum from industrial waste effluents of a cobalt electrodeposition process, *Hydrometallurgy*, 75 (1-4), 77–90.

[30] Ugrina, M., Čeru, T., Nuić, I., and Trgo, M., 2020, Comparative study of mercury(II) removal from aqueous solutions onto natural and iron-modified clinoptilolite rich zeolite, *Processes*, 8 (11), 1523.

[31] Moed, N.M., and Ku, Y., 2022, The effect of Fe(II), Fe(III), Al(III), Ca(II) and Mg(II) on electrocoagulation of As(V), *Water*, 14 (2), 215.

[32] Kim, T., Kim, T.K., and Zoh, K.D., 2020, Removal mechanism of heavy metal (Cu, Ni, Zn, and Cr) in the presence of cyanide during electrocoagulation using Fe and Al electrodes, *J. Water Process Eng.*, 33, 101109.

[33] Du, Z., Gong, Z., Qi, W., Li, E., Shen, J., Li, J., and Zhao, H., 2022, Coagulation performance and floc characteristics of poly-ferric-titanium-silicate-chloride in coking wastewater treatment, *Colloids Surf., A*, 642, 128413.

[34] Li, B., Zhao, J., Ge, W., Li, W., and Yuan, H., 2022, Coagulation-flocculation performance and floc properties for microplastics removal by magnesium hydroxide and PAM, *J. Environ. Chem. Eng.*, 10 (2), 107263.

[35] Saxena, K., and Brighu, U., 2020, Comparison of floc properties of coagulation systems: Effect of particle concentration, scale and mode of flocculation, *J. Environ. Chem. Eng.*, 8 (5), 104311.

[36] Lv, M., Li, D., Zhang, Z., Logan, B.E., Peter van der Hoek, J., Sun, M., Chen, F., and Feng, Y., 2021, Magnetic seeding coagulation: Effect of Al species and magnetic particles on coagulation efficiency, residual Al, and floc properties, *Chemosphere*, 268, 129363.

[37] Lee, S.Y., and Gagnon, G.A., 2016, Growth and structure of flocs following electrocoagulation, *Sep. Purif. Technol.*, 163, 162–168.

[38] Zhang, W., Yao, J., Mu, Y., and Zhang, M., 2023, Electroflocculation of indigo dyeing wastewater from industrial production: Flocs growth and adsorption mechanism, *Arabian J. Chem.*, 16 (12), 105335.

[39] Liu, Y., Liu, Y.Y., Zhang, X., Jiang, W.M., Xiong, W., and Li, J.J., 2024, Study on the treatment of oily wastewater by evaluating the growth process of aggregates in an electrocoagulation reactor, *J. Contam. Hydrol.*, 260, 104269.

[40] He, W., Cheng, X., Huang, Y., Yang, Y., and Lu, J., 2024, The study of the effect of mass transfer of pollutants and flocs on continuous electrocoagulation processes, *Sep. Purif. Technol.*, 329, 125222.

[41] Liu, Y., Zhang, X., Jiang, W., Wu, M., and Li, Z., 2021, Comprehensive review of floc growth and structure using electrocoagulation: Characterization, measurement, and influencing factors, *Chem. Eng. J.*, 417, 129310.

[42] Bharti, M., Das, P.P., and Purkait, M.K., 2023, A review on the treatment of water and wastewater by electrocoagulation process: Advances and emerging applications, *J. Environ. Chem. Eng.*, 11 (6), 111558.

[43] Al-Shannag, M., Al-Qodah, Z., Bani-Melhem, K., Qtaishat, M.R., and Alkasrawi, M., 2015, Heavy metal ions removal from metal plating wastewater using electrocoagulation: Kinetic study and process performance, *Chem. Eng. J.*, 260, 749–756.

[44] Othmani, A., Kesraoui, A., and Seffen, M., 2017, The alternating and direct current effect on the elimination of cationic and anionic dye from aqueous solutions by electrocoagulation and coagulation flocculation, *Euro-Mediterr. J. Environ. Integr.*, 2 (1), 6.

[45] Asaithambi, P., Govindarajan, R., Yesuf, M.B., Selvakumar, P., and Alemayehu, E., 2021, Investigation of direct and alternating current–electrocoagulation process for the treatment of distillery industrial effluent: Studies on operating parameters, *J. Environ. Chem. Eng.*, 9 (2), 104811.

[46] Cerqueira, A.A., Souza, P.S.A., and Marques, M.R.C., 2014, Effects of direct and alternating current on the treatment of oily water in an electroflocculation process, *Braz. J. Chem. Eng.*, 31 (3), 693–701.